frontiers in Medicine

ORIGINAL RESEARCH
published: 15 December 2021
doi: 10.3389/fmed.2021.778346

Macular Vascular Geometry Changes With Sex and Age in Healthy Subjects: A Fundus Photography Study

Ziqing Feng[1†], Gengyuan Wang[1†], Honghui Xia[2†], Meng Li[1], Guoxia Liang[2], Tingting Dong[2], Peng Xiao[1] and Jin Yuan[1*]*

[1] State Key Laboratory of Ophthalmology, Guangdong Provincial Key Laboratory of Ophthalmology and Visual Science, Guangdong Provincial Clinical Research Center for Ocular Diseases, Zhongshan Ophthalmic Center, Sun Yat-sen University, Guangzhou, China, [2] Department of Ophthalmology, Zhaoqing Gaoyao People's Hospital, Zhaoqing, China

OPEN ACCESS

Edited by:
Yu Xiang George Kong, The Royal Victorian Eye and Ear Hospital, Australia

Reviewed by:
Haoyu Chen, Shantou University and the Chinese University of Hong Kong, China
Bo Lei, Henan Provincial People's Hospital, China
Sumit Randhir Singh, University of California, San Diego, United States

***Correspondence:**
Peng Xiao
xiaopengaddis@hotmail.com
Jin Yuan
yuanjincornea@126.com

[†]These authors have contributed equally to this work

Specialty section:
This article was submitted to Ophthalmology, a section of the journal Frontiers in Medicine

Received: *16 September 2021*
Accepted: *17 November 2021*
Published: *15 December 2021*

Citation:
Feng Z, Wang G, Xia H, Li M, Liang G, Dong T, Xiao P and Yuan J (2021) Macular Vascular Geometry Changes With Sex and Age in Healthy Subjects: A Fundus Photography Study. Front. Med. 8:778346. doi: 10.3389/fmed.2021.778346

Purpose: To characterize the sex- and age-related alterations of the macular vascular geometry in a population of healthy eyes using fundus photography.

Methods: A cross-sectional study was conducted with 610 eyes from 305 healthy subjects (136 men, 169 women) who underwent fundus photography examination and was divided into four age groups (G1 with age $\leq$ 25 years, G2 with age 26–35 years, G3 with age 36–45 years, and G4 with age $\geq$ 46 years). A self-developed automated retinal vasculature analysis system allowed segmentation and separate multiparametric quantification of the macular vascular network according to the Early Treatment Diabetic Retinopathy Study (ETDRS). Vessel fractal dimension (D_f), vessel area rate (VAR), average vessel diameter (D_m), and vessel tortuosity (τ_n) were acquired and compared between sex and age groups.

Results: There was no significant difference between the mean age of male and female subjects (32.706 $\pm$ 10.372 and 33.494 $\pm$ 10.620, respectively, $p > 0.05$) and the mean age of both sexes in each age group ($p > 0.05$). The D_f, VAR, and D_m of the inner ring, the D_f of the outer ring, and the D_f and VAR of the whole macula were significantly greater in men than women ($p < 0.001$, $p < 0.001$, $p < 0.05$, respectively). There was no significant change of τ_n between males and females ($p > 0.05$). The D_f, VAR, and D_m of the whole macula, the inner and outer rings associated negatively with age ($p < 0.001$), whereas the τ_n showed no significant association with age ($p > 0.05$). Comparison between age groups observed that D_f started to decrease from G2 compared with G1 in the inner ring ($p < 0.05$) and D_f, VAR, and D_m all decreased from G3 compared with the younger groups in the whole macula, inner and outer rings ($p < 0.05$).

Conclusion: In the healthy subjects, macular vascular geometric parameters obtained from fundus photography showed that D_f, VAR, and D_m are related to sex and age while τ_n is not. The baseline values of the macular vascular geometry were also acquired for both sexes and all age groups.

Keywords: macular vascular geometry, fundus photography, vascular quantification, Early Treatment Diabetic Retinopathy Study (ETDRS), normative baseline

INTRODUCTION

The retina is one of the few tissues in the human body where the blood circulatory system can be non-invasively observed (1, 2). Retinal vascular characteristics can reflect the status of the microcirculation affected by ocular, cardiovascular, and systemic diseases, such as age-related macular degeneration, diabetic retinopathy, Alzheimer's disease, hypertension, etc. (3–11). Since early vascular alterations induced by diseases typically happened in microvasculature (12, 13), changes of the capillaries in the retinal macula are thought to be more sensitive to the early stage of disease progression and could provide significant information for the early diagnosis and monitoring of pathologic changes of related diseases (14–16).

Retinal blood vessels can be observed by imaging techniques such as fundus photography (17), optical coherence tomography angiography (OCTA) (18), fundus fluorescein angiography (FFA) (19), providing abundant retinal vascular structure and perfusion information. While OCTA and FFA could show the more detailed structure and functional changes of microvasculature, FFA is an invasive examination that may induce anaphylactic reactions (20), OCTA provides vascularity of both superficial and deep plexus but is prone to generate artifacts with a scanning imaging regime and its widespread in clinical use and disease screening is limited by the high cost, high patient cooperation and operation difficulties (18, 21). Currently, fundus photography is still the most widely used imaging technique for retinal examination and disease screening due to its advantages of non-invasiveness, relatively low cost, and ease to use the property.

The use of digital image analysis and machine learning techniques for fundus photography has become increasingly common over the past decades (22, 23), offering sophisticated techniques to acquire minute details and quantify the geometry of retinal vascular network (24, 25). Semiautomatic methods developed with Image J (26) and computer-assisted software such as Interactive Vessel Analysis (IVAN), Singapore I Vessel Assessment (SIVA), and Quantitative Analysis of Retinal Vessel Topology and Size (QUARTZ) (25, 27–29) could offer retinal vascular parameters such as vascular length, diameter, tortuosity, and so on. Clinical applications have been conducted showing these parameters may be important indicators of microvascular diseases that can be used in risk prediction (13, 15, 16). Nevertheless, most of the studies focused only on the larger blood vessels around the optic disc (5, 30).

Our former studies have developed a multiparametric retinal vascular network analysis method with a vessel segmentation algorithm based on dense block generative adversarial network (D-GAN) and automated vascular geometry quantification (14, 31). The method has been applied to explore the macular vascular geometry characteristics of fundus photography of patients with diabetes mellitus, showing microvascular morphological parameters may be indicators of the early retinal vessel changes for diabetic retinopathy (14). Though searching for disease-related potential vascular biomarkers is of great importance, the vascular geometry could be different between gender and changes could also be introduced during the normal aging process. While only a few studies have examined the potential sex and age interactions with retinal vasculatures (32, 33), no detailed research has been conducted to quantify the sex- and age-related changes of the microvascular network with fundus photography. In this study, we demonstrated a cross-sectional study aiming to explore the macular vascular geometry variations between sexes and characterized the age-related morphological changes with our multiparametric fundus photography analysis method, finding sensitive indicators of macular vascular geometry changes. Moreover, normative baseline data of both genders in different age groups was provided that can be used as references in identifying progressive macular vascular changes due to different pathologies.

METHODS

Study Subjects

This study was approved by the Medical Ethics Committee, Zhongshan Ophthalmic Center, Sun Yat-sen University (2017KYPJ104), and adhered to the tenets of the Declaration of Helsinki. All the subjects were informed about the data collection and signed informed consent forms. A total of 610 eyes from 305 healthy patients (136 males, 169 females) were recruited from the Zhongshan Ophthalmic Center, Sun Yat-sen University and Zhaoqing Gaoyao People's Hospital, Guangdong province, China between January 1, 2019 and May 15, 2021.

The inclusion criteria were as follows: age 18–70 years old, spherical equivalent within 6.0 diopters (D), no refractive interstitial opacities that affect fundus imaging, intraocular pressure 21 mmHg or less. Ocular examinations included uncorrected and best-corrected visual acuity (BCVA) measurements, digital retinal fundus photography examination with a 50° digital fundus camera (RetiCam 3100, SYSEYE, China) without mydriasis, slit-lamp examination, and intraocular pressure measurement.

The exclusion criteria were BCVA worse than 20/25, history of ocular disease, inflammation, trauma, and any intraocular surgery. Subjects were also excluded if they had any systemic disease, such as diabetes or hypertension that could affect, or are regularly taking any medication.

The subjects were divided into four groups: Group 1 (G1) aged $\leq$ 25 years, Group 2 (G2) aged from 26 to 35 years, Group 3 (G3) aged from 36 to 45 years, and Group 4 (G4) aged $\geq$ 46 years.

Macular Vascular Geometry Multiparametric Measurements

With the color fundus photographs acquired from all the enrolled subjects, multiparametric measurements of the macular vascular geometry were performed with our self-developed fundus photography analysis software. Details of the method could refer to former publications (31). In brief, the fundus image (**Figure 1A**) is first processed by adaptive histogram equalization and bilateral filtering to enhance the contrast between the blood vessels and the background. The enhanced image is then input into a D-GAN-based retinal vascular segmentation algorithm, exporting a binarized retinal vascular network map (**Figure 1B**). The introduction of the dense blocks into the GAN enables more efficient processing between separated spatial regions of

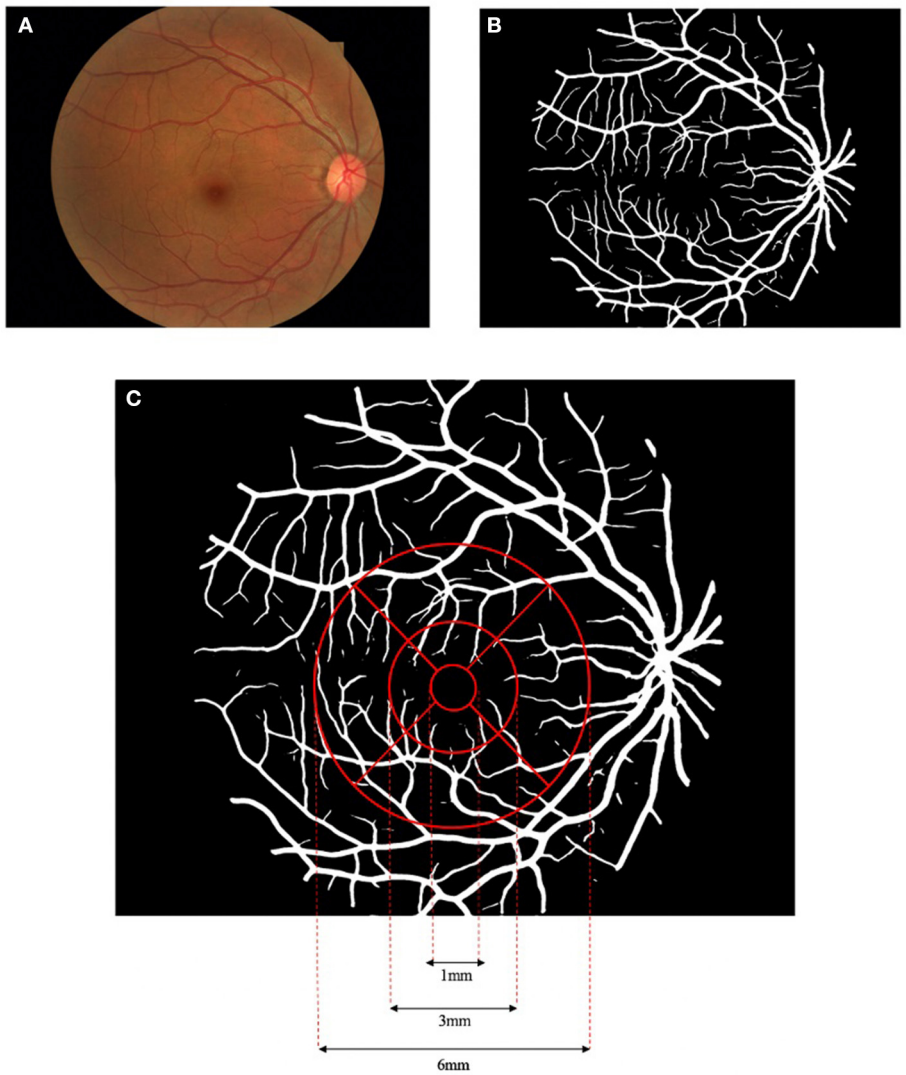

FIGURE 1 | Flowchart of the macular vascular geometry assessment according to Early Treatment Diabetic Retinopathy Study (ETDRS). The fundus photograph **(A)** was pre-processed and input to the dense block generative adversarial network (D-GAN) segmentation system, exporting a binarized retinal vascular network map **(B)**, and further analyzed to quantify the macular vascular geometry based on ETDRS **(C)**.

fundus images, building a more powerful generator to segment smooth, clear, and detailed blood vessels. The segmented vessel network binary image is then further analyzed by our software to quantify the macular vascular geometry based on Early Treatment Diabetic Retinopathy Study (ETDRS), separating the macular area into nine sectors (**Figure 1C**). The diameter of the concentric circles centered at the fovea centers are 1, 3, and 6 mm, respectively, with the inner and outer rings both evenly split into four parts (superior, inferior, nasal, and temporal). Since the innermost circle around the fovea avascular zone seldom has vessels in fundus photographs, this area is excluded for further data analysis. Vascular geometric parameters including fractal dimension (D_f), vessel area rate (VAR), average vessel diameter (D_m), and vessel tortuosity (τ_n) were calculated for both the inner and outer ring as well as their sub-sectors. Note that, D_f is a statistic value calculated with vessel skeletons that describes the space-filling degree of a fractal, measuring the spatial availability of a complex shape, which to some extent can reflect the density and complexity of the selected microvascular network (34–36). VAR is the ratio of the vascular area to the total area of the selected region, which could comprehensively reflect vascular density while D_m is the mean vessel diameter of the vessels in the region. τ_n is defined by multiple subdivision-based algorithms calculating the maximum of the accumulated absolute tangent angle difference of the sub-segments of the blood vessels multiplied by a transformed sigmoid learning curve function of the inflection point numbers of the vessel segment curvature sign, emphasizing the human tortuosity

assessment nature focusing not only global but also on local vascular features (31).

Statistical Analysis

Statistical analysis was performed using Statistical Package for Social Sciences software (SPSS for Mac, version 26.0; IBM SPSS, Inc., Chicago, Illinois, USA). Age and sex were analyzed as classification variables while retinal vascular geometry parameters as continuous variables. Normally or approximately normal distributed variables were summarized as mean ± SD. Retinal vascular geometry parameters were assessed by the Shapiro–Wilk test.

Differences in clinical characteristics between sex at each age group were evaluated using the Independent *t*-test. The ratio of men and women in each group was analyzed by Chi-squared test. Due to the correlation nature of the included binocular data, a generalized estimating equation (GEE) procedure analysis was used with an exchangeable correlation structure to account for the inclusion of both eyes from the same participant. The final GEE model was used to calculate the β coefficients and their 95% CIs. Retinal vascular geometry parameters between the male and female subjects were evaluated through the GEE model. The association of age with D_f, VAR, D_m, and τ_n was examined using a linear GEE model. The differences in age group outcomes were analyzed, gender was included as a covariate. All the *p*-values were 2-sided and considered statistically significant when the values were <0.05.

TABLE 1 | Age and gender characteristics of the studied subjects.

Parameters	Male	Female	*t*-statistic	*p*
Subjects, *n* (eyes)	136 (272)	169 (338)		
Age, Mean ± SD, years	32.706 ± 10.372	33.494 ± 10.620	−0.914	0.361
Age group, Mean ± SD, years				
Group 1 (<25)	22.896 ± 1.525 (*n* = 48)	22.778 ± 1.278 (*n* = 54)	0.601	0.548
Group 2 (26–35)	30.488 ± 2.848 (*n* = 43)	30.904 ± 2.851 (*n* = 52)	−1.000	0.318
Group 3 (36–45)	40.083 ± 3.560 (*n* = 24)	41.121 ± 2.847 (*n* = 33)	−1.669	0.099
Group 4 (>46)	51.238 ± 4.808 (*n* = 21)	52.167 ± 5.063 (*n* = 30)	−0.931	0.354

RESULTS

The general age and gender characteristics of the studied subjects are shown in **Table 1**. There were no significant differences between the mean age of all the male and female subjects (32.706 ± 10.372 and 33.494 ± 10.620, respectively, $p > 0.05$) and the mean ages of both sexes in each age group ($p > 0.05$). Sex ratios were also equally represented in each age group.

Table 2 shows the comparison of macular vascular geometric parameters between all the male and female subjects. **Figure 2** shows the mean ETDRS retinal vascular geometric parameters maps with gender differences. The D_f, VAR, and D_m of the inner ring, the D_f of the outer ring, and the D_f and VAR of the whole macular were significantly greater in males than females (**Table 2**; $p < 0.001$, $p < 0.001$, and $p < 0.05$, respectively), especially in the inferior quadrants (**Figure 2**; $p < 0.001$). There was no significant

TABLE 2 | Generalized estimating equation analysis of the differences of macular vascular geometric parameters between the sex.

	Males	Female	β	95%CI		*p*
				Lower	Upper	
Fractal dimension, Mean ± SD, Df						
Whole	1.397 ± 0.033	1.387 ± 0.036	0.010	0.004	0.017	**0.002****
Inner ring	1,118 ± 0.075	1.087 ± 0.085	0.030	0.015	0.045	**<0.001****
Outer ring	1.318 ± 0.028	1.312 ± 0.031	0.008	0.002	0.013	**0.009****
Vessel area rate, Mean ± SD, VAR						
Whole	0.0141 ± 0.0018	0.0135 ± 0.0021	5.270E−4	1.462E−4	9.081E−4	**0.007****
Inner ring	0.0022 ± 0.0005	0.0020 ± 0.0005	2.391E−4	1.431E−4	3.364E−4	**<0.001****
Outer ring	0.0119 ± 0.0015	0.0116 ± 0.0017	2.850E−4	−3.248E−5	6.023E−4	0.079
Average vessel diameter, Mean ± SD, Dm						
Whole	0.146 ± 0.011	0.146 ± 0.013	4.383E−4	−1.806E−3	2.683E−3	0.702
Inner ring	0.120 ± 0.015	0.115 ± 0.016	0.005	0.002	0.007	**0.001****
Outer ring	0.150 ± 0.012	0.151 ± 0.014	−4.312E−4	−2.850E−3	1.987E−3	0.727
Tortuosity, Mean ± SD, τn						
Whole	2.742 ± 0.147	2.765 ± 0.152	−0.023	−0.051	0.005	0.101
Inner ring	2.945 ± 0.357	2.938 ± 0.359	0.007	−0.052	0.066	0.825
Outer ring	2.688 ± 0.158	2.707 ± 0.171	−0.019	−0.048	0.009	0.189

*p-value was based on GEE analysis using an exchangeable correlation structure for the difference between means, accounting for the correlation between eyes of the same participant. CI, 95% Walder confidence interval; **p < 0.01, bold.*

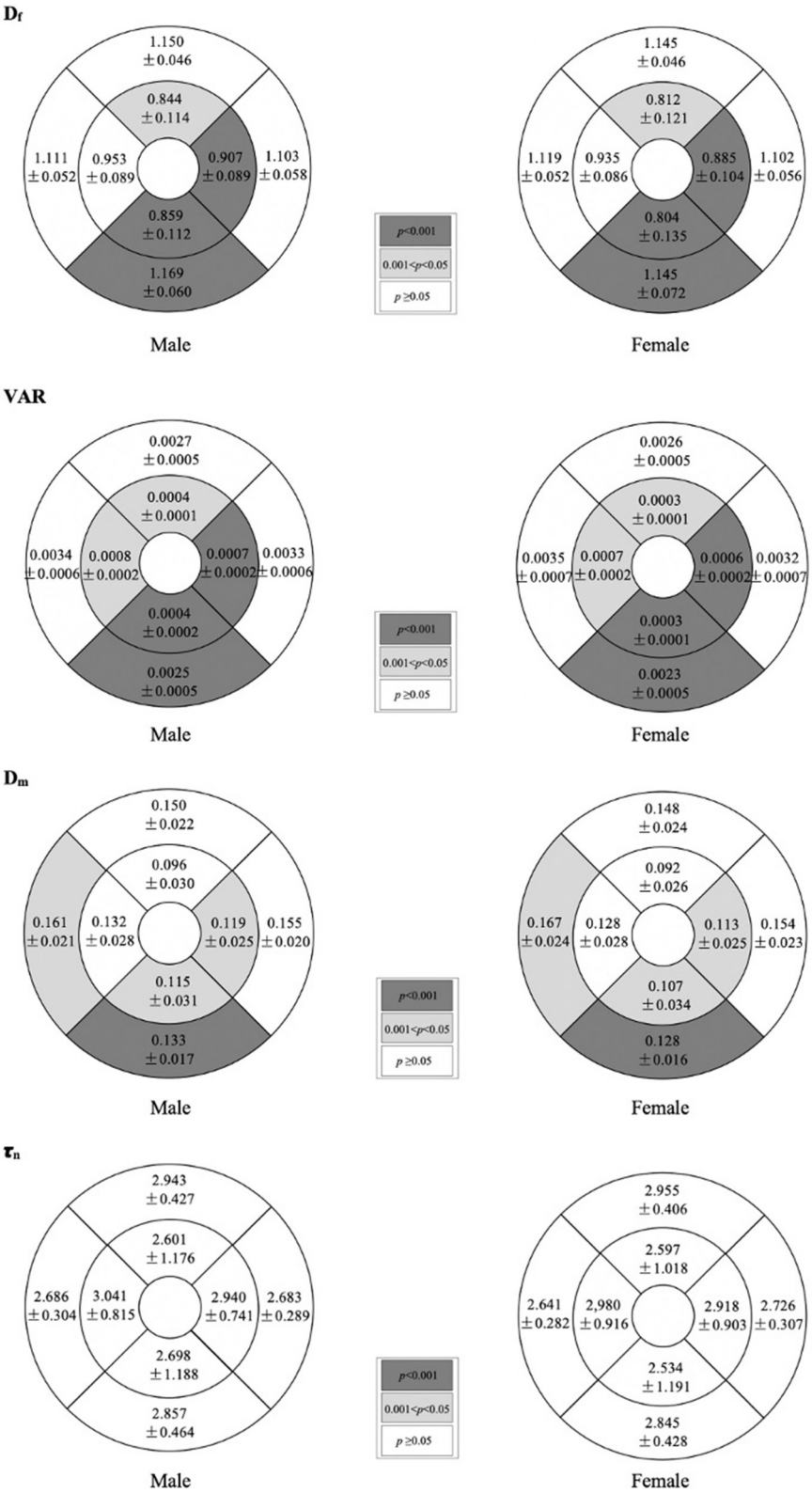

FIGURE 2 | Mean ETDRS retinal vascular geometric parameters maps showing gender differences. Shaded subfields indicate those in which there was a significant difference in macular vascular geometry between the male and female ($p < 0.05$). *p*-value was based on GEE analysis accounting for the correlation between eyes of the same participant.

TABLE 3 | Generalized estimating equation analysis of the association between macular vascular geometric parameters and age.

	Age			
	β	CI		*p*
		Lower	Upper	
Fractal dimension, D_f				
Whole	−9.812E−4	−1.276E−3	−6.873E−4	**<0.001****
Inner ring	−2.069E−3	−2.781E−3	−1.357E−3	**<0.001****
Outer ring	−7.904E−4	−1.043E−3	−5.372E−4	**<0.001****
Vessel area rate, VAR				
Whole	−6.179E−5	−7.804E−5	−4.555E−5	**<0.001****
Inner ring	−1.299E−5	−1.772E−5	−8.264E−5	**<0.001****
Outer ring	−4.873E−5	−6.195E−5	−3.551E−5	**<0.001****
Average vessel diameter, D_m				
Whole	−2.710E−4	−3.741E−4	−1.693E−4	**<0.001****
Inner ring	−2.652E−4	−3.861E−4	−1.440E−4	**<0.001****
Outer ring	−2.684E−4	−3.812E−4	−1.562E−4	**<0.001****
Tortuosity, τ_n				
Whole	7.202E−4	−6.023E−4	2.042E−3	0.286
Inner ring	3.764E−4	−2.734E−3	1.981E−3	0.754
Outer ring	5.203E−4	−7.752E−4	1.815E−3	0.432

p-value was based on GEE analysis using an exchangeable correlation structure for the difference between means, accounting for the correlation between eyes of the same participant.
*CI, 95% Walder confidence interval; **p < 0.01, bold.*

difference of τ_n between males and females (**Table 2**; **Figure 2**; $p > 0.05$).

Table 3 shows the association results between macular vascular geometric parameters and age. The D_f, VAR, and D_m of the whole macular, inner and outer rings all negatively associated with age (**Table 3**; **Figure 3**; $p < 0.001$), whereas the τ_n of the macular did not correlate with age (**Table 3**; **Figure 3**; $p > 0.05$).

The comparison of macular vascular geometric parameters of the whole, the inner and the outer rings among the different age groups are shown in **Figure 4**. It is resolved that, in the inner ring, G2 showed a significant decrease of the D_f compared with G1 (**Figure 4**; $p < 0.05$), while D_f, VAR, and D_m all decreased from G3 compared with the younger groups in the whole, inner and outer rings (**Figure 4**; $p < 0.05$). τn also has no significant differences (**Figure 4**; $p > 0.05$).

Table 4 shows the baseline values of D_f, VAR, D_m, and τ_n of both sexes in 4 age groups.

DISCUSSION

This is the first study that quantifies the sex- and age-related macular vascular geometry alterations in healthy populations with fundus photography using our customized automatic multiparametric vascular analysis software. We demonstrated that macular vascular D_f, VAR, and average vessel diameter D_m were all significantly lower in the female than male and all decrease with the increase of age, while vessel tortuosity τ_n showed no statistical difference, revealing the physiological variations of macular vascular geometry induced by sex and age. Normative baseline data of macular vascular geometric parameters for both the genders in different age groups were acquired that can potentially be used as references in identifying progressive macular vascular changes due to different pathologies.

In the analysis of the macular vascular geometric difference between male and female healthy subjects, we found that D_f and VAR in the macular area and D_m in the inner area of the macula were significantly greater in men than in women, indicating that male has more complex retinal vascular structures and larger vessel occupation and diameter in the macular area as compared with female. While no studies have demonstrated macular vascular structure analysis with fundus photography between genders, our results showing more abundant vascular network in men are in consistent with the former studies. Using OCTA, Yu et al. (37) reported lower blood flow index in the macula and larger fovea avascular zone in women, and Wang et al. (38) revealed higher superficial retinal vascular density in men than in women. Using fundus photography, Tapp et al. (39) showed that the retinal vascular diameter around the optic disk was larger in male. Since the retina is a tissue with high-oxygen consumption that need to rely on blood perfusion to maintain its metabolic levels, the retinal vascular structure is mainly influenced by the blood perfusion level (37, 40), which is regulated by blood pressure, intraocular pressure (IOP) (41), body mass index (BMI) (42), and hormone (43). Thus, the proven differences in these factors between genders (44) might be the reasons leading to the macular vascular geometry divergence. There were studies exploring gender differences in the epidemiology of ophthalmic diseases that have shown that macular diseases such as age-related macular degeneration (AMD) and macular holes (45, 46) were more likely to happen in females, which could also potentially be related to the macular vascular geometry differences. The detailed mechanisms of the gender-specific differences of macular vascular geometry remain unclear and require further study.

We have described the association between age and macular vascular geometric parameters showing that D_f, VAR, and D_m of the macular area all decrease with the increase of age. The association between age and D_f, VAR, and D_m were significant while the correlation coefficient is relatively low, indicating small age-related macular vascular geometry changes. This is similar to those reported in other studies (47, 48). One possible reason is that the age range of the samples in our study is not wide enough with the fewer elderly samples. The other reason could be that many factors influence macular vessels such as gender, axial length, refractive error (47, 49, 50), while this study limited in exploring only the age-induced changes. In the comparison of macular vascular geometric parameters of different age groups, we have revealed that statistical variation of vascular D_f happened from 26 to 35 age group while VAR and D_m decrease from 36 to 45 age group. These are in accordance with studies demonstrated in exploring retinal vascular alterations with aging (34, 51). Using fundus photography, Azemin et al. (51) and Liew et al. (34) measured the whole retinal and observed a significant decrease

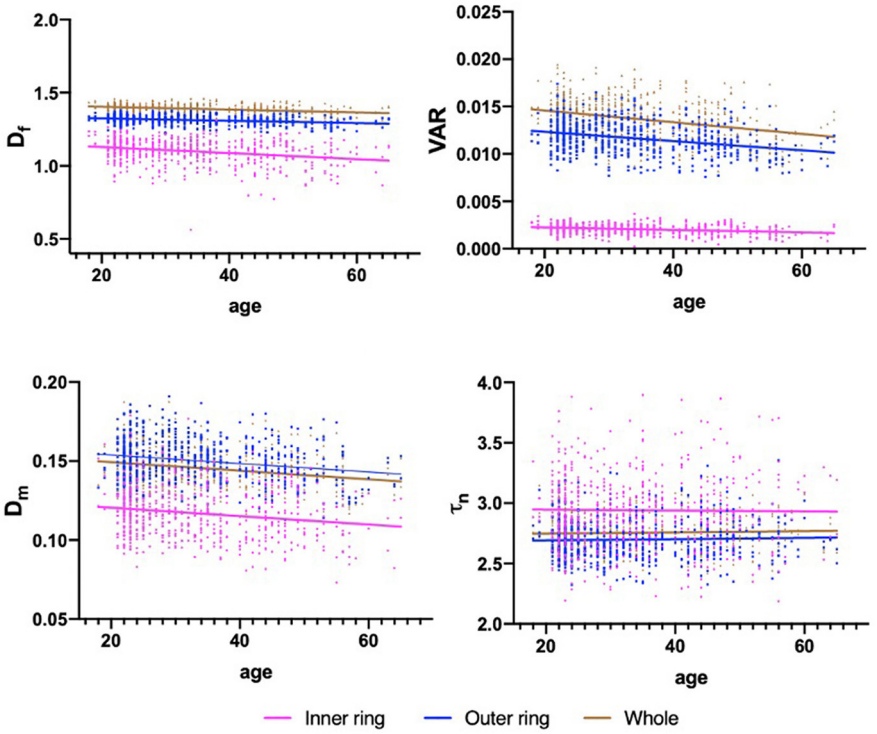

FIGURE 3 | Scatterplots for the associations between macular vascular parameters and age. The significant negative association exists between the D_f, VAR, D_m, and age in the whole macula, inner and outer rings ($p < 0.001$), while τ_n showed no significant association with age ($p > 0.05$).

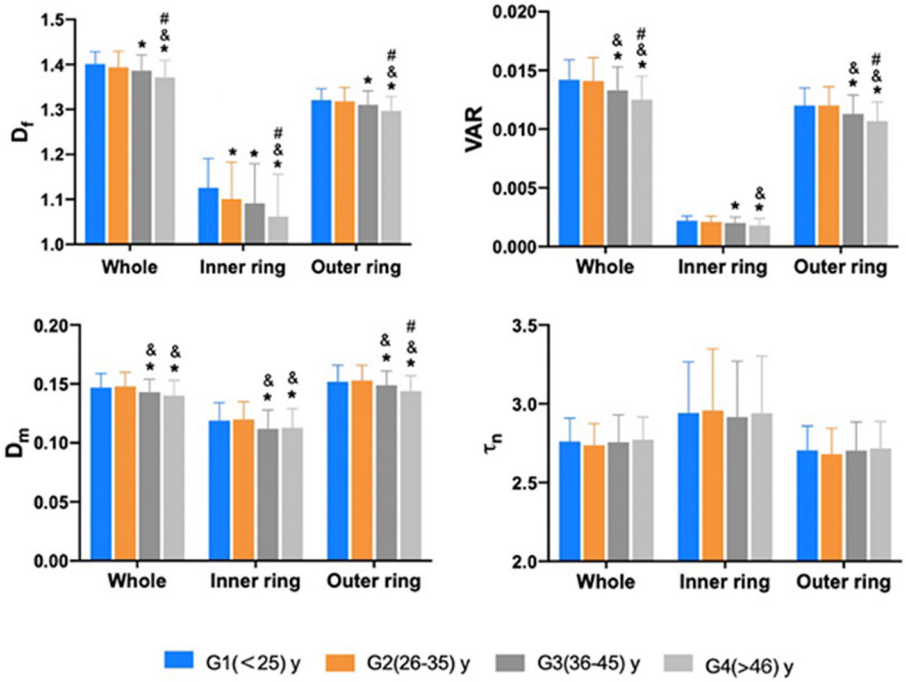

FIGURE 4 | The comparison of macular vascular geometric parameters of the whole, the inner and outer rings among different age groups. Df of the inner ring showed a significant decrease in G2 compared to G1 ($p < 0.05$). D_f, VAR, and D_m all decreased from G3 compared to younger groups in the whole, inner and outer rings ($p < 0.05$). τn has no significant differences ($p > 0.05$). *Compare to G1 $p < 0.05$; $^{\&}$ compare to G2 $p < 0.05$; $^{\#}$: compare to G3 $p < 0.05$. p value was based on GEE analysis accounting for the correlation between eyes of the same participant and including gender as a covariate.

TABLE 4 | The baseline values of macular vascular geometric parameters of both the sexes in the four age groups.

Age groups	Group 1		Group 2		Group 3		Group 4	
	Male	Female	Male	Female	Male	Female	Male	Female
Fractal dimension, Mean ± SD, D_f								
Whole	1.400 ± 0.027	1.401 ± 0.027	1.399 ± 0.032	1.390 ± 0.038	1.398 ± 0.036	1.378 ± 0.032	1.382 ± 0.038	1.363 ± 0.037
Inner ring	1.128 ± 0.068	1.124 ± 0.061	1.116 ± 0.074	1.088 ± 0.086	1.127 ± 0.081	1.065 ± 0.083	1.090 ± 0.080	1.043 ± 0.099
Outer ring	1.320 ± 0.024	1.322 ± 0.027	1.321 ± 0.027	1.315 ± 0.033	1.318 ± 0.032	1.304 ± 0.029	1.307 ± 0.033	1.290 ± 0.030
Vessel area rate, Mean ± SD, VAR								
Whole	0.0142 ± 0.0016	0.0143 ± 0.0018	0.0144 ± 0.0018	0.0139 ± 0.0020	0.0140 ± 0.0019	0.0129 ± 0.0019	0.0133 ± 0.0021	0.0120 ± 0.0018
Inner ring	0.0023 ± 0.0005	0.0022 ± 0.0004	0.0022 ± 0.0005	0.0020 ± 0.0005	0.0022 ± 0.0005	0.0018 ± 0.0005	0.0021 ± 0.0005	0.0017 ± 0.0006
Outer ring	0.0119 ± 0.0014	0.0121 ± 0.0016	0.0122 ± 0.0015	0.0119 ± 0.0017	0.0117 ± 0.0015	0.0110 ± 0.0016	0.0112 ± 0.0017	0.0103 ± 0.0014
Average vessel diameter, Mean ± SD, D_m								
Whole	0.145 ± 0.011	0.149 ± 0.013	0.149 ± 0.011	0.148 ± 0.012	0.145 ± 0.011	0.142 ± 0.011	0.142 ± 0.011	0.139 ± 0.013
Inner ring	0.121 ± 0.016	0.117 ± 0.014	0.123 ± 0.014	0.117 ± 0.016	0.117 ± 0.014	0.109 ± 0.016	0.115 ± 0.014	0.111 ± 0.017
Outer ring	0.149 ± 0.012	0.154 ± 0.015	0.153 ± 0.012	0.152 ± 0.013	0.151 ± 0.0119	0.147 ± 0.0126	0.146 ± 0.012	0.143 ± 0.014
Tortuosity, Mean ± SD, τ_n								
Whole	2.757 ± 0.144	2.765 ± 0.151	2.729 ± 0.143	2.745 ± 0.134	2.737 ± 0.164	2.769 ± 0.183	2.743 ± 0.141	2.794 ± 0.142
Inner ring	2.921 ± 0.300	2.961 ± 0.343	2.990 ± 0.468	2.930 ± 0.308	2.910 ± 0.291	2.918 ± 0.397	2.945 ± 0.257	2.938 ± 0.425
Outer ring	2.709 ± 0.148	2.701 ± 0.161	2.662 ± 0.158	2.697 ± 0.167	2.694 ± 0.183	2.710 ± 0.180	2.691 ± 0.149	2.735 ± 0.184

in the D_f with aging. Sun et al. (52) found both arterial and venular caliber decrease in the older groups using IVAN software to analyze peripapillary diameter of 3,019 health participants; Pose-Reino et al. (53) analyzed the retinal blood vessel caliber and found that the reduction of retinal arteriole caliber occurs during aging. While the retinal vascular structure is closely related to blood perfusion, measuring by OCTA, Yu et al. (37) have shown that macular perfusion decreased with increasing age in healthy Chinese eyes, and the parafoveal flow index and vessel area density decrease with aging at a rate of 0.6 and 0.4% per year. You et al. also reported that higher superficial and deep capillary densities were significantly associated with younger age and a general negative association between macular vessel density and age (47). Similar results have been reported in several other studies (48). Similar to other human organs, the physiological function of the eye decreases with aging. Since maintaining normal function of the retina depends on normal metabolism level (54), aging causes tissue loss and a corresponding reduction in oxygen demand, altering vascular system, and declining the perfusion of macular, resulting in a reduction in vascular structure and complexity. Studies have also determined that aging could cause thickening of the vascular wall, reducing vascular elasticity (55), and the rigidity of the vessel wall would lead to the decrease of the vessel diameter (56). The reduction in the macular vascular structure might potentially account for some ocular diseases related to age such as age-related macular degeneration (AMD), proliferative diabetic retinopathy (PDR), retinal vein occlusion (RVO), and so on (57, 58).

In this study, we also found that the macular vascular tortuosity τ_n has no variation between gender and across aging. Many studies have shown that retinal vascular tortuosity variation is one of the earliest indicators of a number of relevant diseases such as diabetes, cerebrovascular disease, stroke, ischemic heart disease (14, 59, 60). Our observation indicates no statistical difference of macular vascular tortuosity in healthy individuals of different gender and age further enhancing the feasibility of using tortuosity as a sensitive indicator for the early diagnosis of related diseases.

There are several limitations of this study. First, the number of subjects in the elderly age group was relatively small due to the fact that the healthy subjects we have collected tend to be young since older people are more likely to suffer from systemic diseases such as hypertension, heart disease, and diabetes or cloudy refractive interstitium affecting the fundus image quality (6, 9, 14, 34, 50). Future collection of more healthy elderly subjects to balance the sample size of all the age groups would be beneficial. Second, while this study is limited in exploring macular vascular geometry changes with age and gender, there are many other factors that affect the macular vasculature, such as axial length, refractive error, IOP, blood pressure, and so on (34, 41, 49, 50, 61), it is worth further in-depth study considering these factors. Third, since this is a cross-sectional study without temporal information, future prospective investigation with systematic clinical information acquired could provide more detailed support of the vascular alteration mechanisms. Moreover, with the binocular data acquired in this study, analyzing the intereye correlation and difference of the macular vasculature with fundus photography and comparing it to those acquired with OCTA would be interesting (62). Finally, with the baseline data from the healthy subjects gained, the vascular geometric variation induced by different diseases could be further explored. Improvement of our current vascular analysis software to distinguish the retinal arteries and veins would also provide more functional information to study the retinal vascular circulation.

In conclusion, findings from this study reveal the sex- and age-related macular vascular geometry alterations in healthy human subjects and provide the normative baseline data for both genders in different age groups. The application of our automatic retinal vascular analysis system could provide a useful approach for detecting subtle macular vessels change with fundus photography.

DATA AVAILABILITY STATEMENT

The original contributions presented in the study are included in the article/supplementary material, further inquiries can be directed to the corresponding authors.

ETHICS STATEMENT

The studies involving human participants were reviewed and approved by Guangzhou, China 2017KYPJ104, Medical Ethics Committee of Zhongshan Ophthalmic Center, Sun Yat-sen University (Guangzhou, China). Written informed consent to participate in this study was provided by the participants' legal guardian/next of kin.

AUTHOR CONTRIBUTIONS

JY and PX conceived and planned the research and reviewed and modified the manuscript. ZF, GW, and HX carried out the studies and wrote the first draft of the manuscript. GL and TD conducted the fundus imaging. GW, PX, and ML processed the images and organized the database. ZF and GL performed the statistical analysis. All the authors provided critical feedback and helped to shape the research, analysis, and manuscript.

FUNDING

This study was supported by the Key-Area Research and Development Program of Guangdong Province (No. 2019B010152001), the National Natural Science Foundation of China (81901788), and the Guangzhou Science and Technology Program (202002030412).

REFERENCES

1. Flammer J, Konieczka K, Bruno RM, Virdis A, Flammer AJ, Taddei S. The eye and the heart. *Eur Heart J.* (2013) 34:1270–8. doi: 10.1093/eurheartj/eht023
2. Liew G, Wang JJ, Mitchell P, Wong TY. Retinal vascular imaging: a new tool in microvascular disease research. *Circ Cardiovasc Imaging.* (2008) 1:156–61. doi: 10.1161/CIRCIMAGING.108.784876
3. Parisi V, Ziccardi L, Costanzo E, Tedeschi M, Barbano L, Manca D, et al. Macular functional and morphological changes in intermediate age-related maculopathy. *Invest Ophthalmol Vis Sci.* (2020) 61:11. doi: 10.1167/iovs.61.5.11
4. Ozcaliskan S, Artunay O, Balci S, Perente I, Yenerel NM. Quantitative analysis of inner retinal structural and microvascular alterations in intermediate age-related macular degeneration: a swept-source OCT angiography study. *Photodiagnosis Photodyn Ther.* (2020) 32:102030. doi: 10.1016/j.pdpdt.2020.102030
5. Liew G, Benitez-Aguirre P, Craig ME, Jenkins AJ, Hodgson LAB, Kifley A, et al. Progressive retinal vasodilation in patients with type 1 diabetes: a longitudinal study of retinal vascular geometry. *Invest Ophthalmol Vis Sci.* (2017) 58:2503–09. doi: 10.1167/iovs.16-21015
6. Lim LS, Chee ML, Cheung CY, Wong TY. Retinal vessel geometry and the incidence and progression of diabetic retinopathy. *Invest Ophthalmol Vis Sci.* (2017) 58:200–5. doi: 10.1167/iovs.17-21699
7. Berisha F, Feke GT, Trempe CL, McMeel JW, Schepens CL. Retinal abnormalities in early Alzheimer's disease. *Invest Ophthalmol Vis Sci.* (2007) 48:2285–9. doi: 10.1167/iovs.06-1029
8. Golzan SM, Goozee K, Georgevsky D, Avolio A, Chatterjee P, Shen K, et al. Retinal vascular and structural changes are associated with amyloid burden in the elderly: ophthalmic biomarkers of preclinical Alzheimer's disease. *Alzheimers Res Ther.* (2017) 9:13. doi: 10.1186/s13195-017-0239-9
9. Chua J, Chin CWL, Hong J, Chee ML, Le TT, Ting DSW, et al. Impact of hypertension on retinal capillary microvasculature using optical coherence tomographic angiography. *J Hypertens.* (2019) 37:572–80. doi: 10.1097/HJH.0000000000001916
10. Liu M, Lycett K, Moreno-Betancur M, Wong TY, He M, Saffery R, et al. Inflammation mediates the relationship between obesity and retinal vascular calibre in 11-12 year-olds children and mid-life adults. *Sci Rep.* (2020) 10:5006. doi: 10.1038/s41598-020-61801-w
11. Ong YT, De Silva DA, Cheung CY, Chang HM, Chen CP, Wong MC, et al. Microvascular structure and network in the retina of patients with ischemic stroke. *Stroke.* (2013) 44:2121–7. doi: 10.1161/STROKEAHA.113.001741
12. Durham JT, Herman IM. Microvascular modifications in diabetic retinopathy. *Curr Diab Rep.* (2011) 11:253–64. doi: 10.1007/s11892-011-0204-0
13. Witt N, Wong TY, Hughes AD, Chaturvedi N, Klein BE, Evans R, et al. Abnormalities of retinal microvascular structure and risk of mortality from ischemic heart disease and stroke. *Hypertension.* (2006) 47:975–81. doi: 10.1161/01.HYP.0000216717.72048.6c
14. Li M, Wang G, Xia H, Feng Z, Xiao P, Yuan J. Retinal vascular geometry detection as a biomarker in diabetes mellitus. *Eur J Ophthalmol.* (2021) 20:11206721211033488. doi: 10.1177/11206721211033488
15. Chen Q, Tan F, Wu Y, Zhuang X, Wu C, Zhou Y, et al. Characteristics of retinal structural and microvascular alterations in early type 2 diabetic patients. *Invest Ophthalmol Vis Sci.* (2018) 59:2110–8. doi: 10.1167/iovs.17-23193
16. Jiang H, Wei Y, Shi Y, Wright CB, Sun X, Gregori G, et al. Altered macular microvasculature in mild cognitive impairment and Alzheimer disease. *J Neuroophthalmol.* (2018) 38:292–8. doi: 10.1097/WNO.0000000000000580
17. Sinthanayothin C, Boyce JF, Cook HL, Williamson TH. Automated localisation of the optic disc, fovea, and retinal blood vessels from digital colour fundus images. *Br J Ophthalmol.* (1999) 83:902–10. doi: 10.1136/bjo.83.8.902
18. Spaide RF, Fujimoto JG, Waheed NK, Sadda SR, Staurenghi G. Optical coherence tomography angiography. *Prog Retin Eye Res.* (2018) 64:1–55. doi: 10.1016/j.preteyeres.2017.11.003
19. Manivannan A, Plskova J, Farrow A, Mckay S, Sharp PF, Forrester JV. Ultra-wide-field fluorescein angiography of the ocular fundus. *Am J Ophthalmol.* (2005) 140:525–7. doi: 10.1016/j.ajo.2005.02.055
20. Kornblau IS, El-Annan JF. Adverse reactions to fluorescein angiography: a comprehensive review of the literature. *Surv Ophthalmol.* (2019) 64:679–93. doi: 10.1016/j.survophthal.2019.02.004
21. Chalam KV, Sambhav K. Optical coherence tomography angiography in retinal diseases. *J Ophthalmic Vis Res.* (2016) 11:84–92. doi: 10.4103/2008-322X.180709
22. Silva PS, Cavallerano JD, Sun JK, Noble J, Aiello LM, Aiello LP. Nonmydriatic ultrawide field retinal imaging compared with dilated standard 7-field 35-mm photography and retinal specialist examination for evaluation of diabetic retinopathy. *Am J Ophthalmol.* (2012) 154:549–559.e2. doi: 10.1016/j.ajo.2012.03.019
23. Gulshan V, Peng L, Coram M, Stumpe MC, Wu D, Narayanaswamy A, et al. Development and validation of a deep learning algorithm for detection of diabetic retinopathy in retinal fundus photographs. *JAMA.* (2016) 316:2402–10. doi: 10.1001/jama.2016.17216

24. Thomas GN, Ong SY, Tham YC, Hsu W, Lee ML, Lau QP, et al. Measurement of macular fractal dimension using a computer-assisted program. *Invest Ophthalmol Vis Sci.* (2014) 55:2237–43. doi: 10.1167/iovs.13-13315
25. Zheng Y, Cheung N, Aung T, Mitchell P, He M, Wong TY. Relationship of retinal vascular caliber with retinal nerve fiber layer thickness: the Singapore Malay eye study. *Invest Ophthalmol Vis Sci.* (2009) 50:4091–6. doi: 10.1167/iovs.09-3444
26. Olga GS, Svetlana F, Mikhail S, Igor Z. Evaluation of vascular system of the retina using ImageJ software. *Invest Ophthalmol Vis Sci.* (2011) 52:1281.
27. Lim LS, Cheung CY, Sabanayagam C, Lim SC, Tai ES, Huang L, et al. Structural changes in the retinal microvasculature and renal function. *Invest Ophthalmol Vis Sci.* (2013) 54:2970–6. doi: 10.1167/iovs.13-11941
28. Welikala RA, Fraz MM, Foster PJ, Whincup PH, Rudnicka AR, Owen CG, et al. UK Biobank Eye and Vision Consortium. Automated retinal image quality assessment on the UK Biobank dataset for epidemiological studies. *Comput Biol Med.* (2016) 71:67–76. doi: 10.1016/j.compbiomed.2016.01.027
29. Bankhead P, Scholfield CN, McGeown JG, Curtis TM. Fast retinal vessel detection and measurement using wavelets and edge location refinement. *PLoS One.* (2012) 7:e32435. doi: 10.1371/journal.pone.0032435
30. Cheung CY, Sabanayagam C, Law AK, Kumari N, Ting DS, Tan G, et al. Retinal vascular geometry and 6 year incidence and progression of diabetic retinopathy. *Diabetologia.* (2017) 60:1770–81. doi: 10.1007/s00125-017-4333-0
31. Wang G, Li M, Yun Z, Duan Z, Ma K, Luo Z, et al. novel multiple subdivision-based algorithm for quantitative assessment of retinal vascular tortuosity. *Exp Biol Med.* (2021) 246:2222–9. doi: 10.1177/15353702211032898
32. Benitez-Aguirre P, Craig ME, Cass HG, Sugden CJ, Jenkins AJ, Wang JJ, et al. Sex differences in retinal microvasculature through puberty in type 1 diabetes: are girls at greater risk of diabetic microvascular complications? *Invest Ophthalmol Vis Sci.* (2014) 56:571–7. doi: 10.1167/iovs.14-15147
33. Huang QF, Wei FF, Zhang ZY, Raaijmakers A, Asayama K, Thijs L, et al. Reproducibility of retinal microvascular traits decoded by the Singapore I vessel assessment software across the human age range. *Am J Hypertens.* (2018) 31:438–49. doi: 10.1093/ajh/hpx202
34. Liew G, Wang JJ, Cheung N, Zhang YP, Hsu W, Lee ML, et al. The retinal vasculature as a fractal: methodology, reliability, and relationship to blood pressure. *Ophthalmology.* (2008) 115:1951–6. doi: 10.1016/j.ophtha.2008.05.029
35. Azemin MZ, Kumar DK, Wong TY, Kawasaki R, Mitchell P, Wang JJ. Robust methodology for fractal analysis of the retinal vasculature. *IEEE Trans Med Imaging.* (2011) 30:243–50. doi: 10.1109/TMI.2010.2076322
36. Masters BR. Fractal analysis of the vascular tree in the human retina. *Annu Rev Biomed Eng.* (2004) 6:427–52. doi: 10.1146/annurev.bioeng.6.040803.140100
37. Yu J, Jiang C, Wang X, et al. Macular perfusion in healthy Chinese: an optical coherence tomography angiogram study. *Invest Ophthalmol Vis Sci.* (2015) 56:3212–7. doi: 10.1167/iovs.14-16270
38. Wang Q, Chan S, Yang JY, You B, Wang YX, Jonas JB, et al. Vascular density in retina and choriocapillaris as measured by optical coherence tomography angiography. *Am J Ophthalmol.* (2016) 168:95–109. doi: 10.1016/j.ajo.2016.05.005
39. Tapp RJ, Owen CG, Barman SA, Welikala RA, Foster PJ, Whincup PH, et al. UK Biobank Eye, Vision Consortium. Retinal vascular tortuosity and diameter associations with adiposity and components of body composition. *Obesity.* (2020) 28:1750–60. doi: 10.1002/oby.22885
40. Yu DY, Cringle SJ. Oxygen distribution and consumption within the retina in vascularised and avascular retinas and in animal models of retinal disease. *Prog Retin Eye Res.* (2001) 20:175–208. doi: 10.1016/S1350-9462(00)00027-6
41. Alagoz G, Gurel K, Bayer A, Serin D, Celebi S, Kukner S, et al. comparative study of bimatoprost and travoprost: effect on intraocular pressure and ocular circulation in newly diagnosed glaucoma patients. *Ophthalmologica.* (2008) 222:88–95. doi: 10.1159/000112624
42. Hughes AD, Wong TY, Witt N, Evans R, Thom SA, Klein BE, et al. Determinants of retinal microvascular architecture in normal subjects. *Microcirculation.* (2009) 16:159–66. doi: 10.1080/10739680802353868
43. Nuzzi R, Scalabrin S, Becco A, Panzica G. Gonadal hormones and retinal disorders: a review. *Front Endocrinol.* (2018) 9:66. doi: 10.3389/fendo.2018.00066
44. Schmidl D, Schmetterer L, Garhöfer G, Popa-Cherecheanu A. Gender differences in ocular blood flow. *Curr Eye Res.* (2015) 40:201–12. doi: 10.3109/02713683.2014.906625
45. Rudnicka AR, Jarrar Z, Wormald R, Cook DG. Fletcher A, Owen CG. Age and gender variations in age-related macular degeneration prevalence in populations of European ancestry: a meta-analysis. *Ophthalmology.* (2012) 119:571–80. doi: 10.1016/j.ophtha.2011.09.027
46. McCannel CA, Ensminger JL, Diehl NN, Hodge DN. Population-based incidence of macular holes. *Ophthalmology.* (2009) 116:1366–9. doi: 10.1016/j.ophtha.2009.01.052
47. You QS, Chan JCH, Ng ALK, Choy BKN, Shih KC, Cheung JJC, et al. Macular vessel density measured with optical coherence tomography angiography and its associations in a large population-based study. *Invest Ophthalmol Vis Sci.* (2019) 60:4830–7. doi: 10.1167/iovs.19-28137
48. Wei Y, Jiang H, Shi Y, Qu D, Gregori G, Zheng F, et al. Age-related alterations in the retinal microvasculature, microcirculation, and microstructure. *Invest Ophthalmol Vis Sci.* (2017) 58:3804–17. doi: 10.1167/iovs.17-21460
49. Fernández-Vigo JI, Kudsieh B, Shi H, Arriola-Villalobos P, Donate-López J, García-Feijóo J, et al. Normative database and determinants of macular vessel density measured by optical coherence tomography angiography. *Clin Exp Ophthalmol.* (2020) 48:44–52. doi: 10.1111/ceo.13648
50. Cheung CY, Thomas GN, Tay W, Ikram MK, Hsu W, Lee ML, et al. Retinal vascular fractal dimension and its relationship with cardiovascular and ocular risk factors. *Am J Ophthalmol.* (2012) 154:663–74. doi: 10.1016/j.ajo.2012.04.016
51. Azemin MZ, Kumar DK, Wong TY, Wang JJ, Mitchell P, Kawasaki R, et al. Age-related rarefaction in the fractal dimension of retinal vessel. *Neurobiol Aging.* (2012) 33:194.e1–4. doi: 10.1016/j.neurobiolaging.2010.04.010
52. Sun C, Liew G, Wang JJ, Mitchell P, Saw SM, Aung T, et al. Retinal vascular caliber, blood pressure, and cardiovascular risk factors in an Asian population: the Singapore Malay Eye Study. *Invest Ophthalmol Vis Sci.* (2008) 49:1784–90. doi: 10.1167/iovs.07-1450
53. Pose-Reino A, Gomez-Ulla F, Hayik B, Rodriguez-Fernández M, Carreira-Nouche MJ, Mosquera-González A, et al. Computerized measurement of retinal blood vessel calibre: description, validation and use to determine the influence of ageing and hypertension. *J Hypertens.* (2005) 23:843–50. doi: 10.1097/01.hjh.0000163154.35577.8e
54. Vandewalle E, Abegão Pinto L, Olafsdottir OB, De Clerck E, Stalmans P. Van Calster J, et al. Oximetry in glaucoma: correlation of metabolic change with structural and functional damage. *Acta Ophthalmol.* (2014) 92:105–10. doi: 10.1111/aos.12011
55. Meixner E, Michelson G. Measurement of retinal wall-tolumen ratio by adaptive optics retinal camera: a clinical research. *Graefes Arch Clin Exp Ophthalmol.* (2015) 253:1985–95. doi: 10.1007/s00417-015-3115-y
56. Wong TY, Klein R, Klein BE, Tielsch JM, Hubbard L, Nieto FJ. Retinal microvascular abnormalities and their relationship with hypertension, cardiovascular disease, and mortality. *Surv Ophthalmol.* (2001) 46:59–80. doi: 10.1016/S0039-6257(01)00234-X
57. Kromer R, Glusa P, Framme C, Pielen A, Junker B. Optical coherence tomography angiography analysis of macular flow density in glaucoma. *Acta Ophthalmol.* (2019) 97:e199–206. doi: 10.1111/aos.13914
58. Seknazi D, Coscas F, Sellam A, Rouimi F, Coscas G, Souied EH, et al. Optical coherence tomography angiography in retinal vein occlusion: correlations between macular vascular density, visual acuity, and peripheral nonperfusion area on fluorescein angiography. *Retina.* (2018) 38:1562–70. doi: 10.1097/IAE.0000000000001737
59. Cheung CY, Zheng Y, Hsu W, Lee ML, Lau QP, Mitchell P, et al. Retinal vascular tortuosity, blood pressure, and cardiovascular risk factors. *Ophthalmology.* (2011) 118:812–8. doi: 10.1016/j.ophtha.2010.08.045
60. Sasongko MB, Wong TY, Nguyen TT, Cheung CY, Shaw JE, Wang JJ. Retinal vascular tortuosity in persons with diabetes and diabetic retinopathy. *Diabetologia.* (2011) 54:2409–16. doi: 10.1007/s00125-011-2200-y
61. Zhang J, Tang FY, Cheung CY, Chen H. Different effect of media opacity on vessel density measured by different optical coherence tomography angiography algorithms. *Transl Vis Sci Technol.* (2020) 9:19. doi: 10.1167/tvst.9.8.19
62. Fang D, Tang FY, Huang H, Cheung CY, Chen H. Repeatability, interocular correlation and agreement of quantitative swept-source optical

coherence tomography angiography macular metrics in healthy subjects. *Br J Ophthalmol.* (2019) 103:415–20. doi: 10.1136/bjophthalmol-2018-311874

Conflict of Interest: The authors declare that the research was conducted in the absence of any commercial or financial relationships that could be construed as a potential conflict of interest.

Publisher's Note: All claims expressed in this article are solely those of the authors and do not necessarily represent those of their affiliated organizations, or those of the publisher, the editors and the reviewers. Any product that may be evaluated in this article, or claim that may be made by its manufacturer, is not guaranteed or endorsed by the publisher.